PROCEEDINGS OF SCIENCE

GRB 130831A: birth and death of a magnetar at z = 0.5

M. De Pasquale[1,2*], S. R. Oates[2,3], J. L. Racusin[4], D. A. Kann[5], B. Zhang[6], A. Pozanenko[7], A. A. Volnova[7], A. Trotter[8], N. Frank[8], A. Cucchiara[4], E. Troja[4], B. Sbarufatti[9], N. R. Butler[10], S. Schulze[11,12], Z. Cano[13], M. J. Page[2], A. J. Castro-Tirado[3], J. Gorosabel[3,14,15], A. Lien[4,16], O. D. Fox[17], O. Littlejohns[10], J. S. Bloom[17], J. X. Prochaska[18], J. A. de Diego[18], J. Gonzalez[19], M. G. Richer[19], C. Román-Zúñiga[19], A. M. Watson[19], N. Gehrels[4], H. Moseley[4], A. Kutyrev[4], S. Zane[2], V. Hoette[20], R. R. Russell[20], V. Rumyantsev[21], E. Klunko[22], O. Burkhonov[23], A. A. Breeveld[2], D. E. Reichart[8], J.B. Haislip[8]

[1]*Mullard Space Science Laboratory, University College London, Dorking, United Kingdom*
[2]*Istituto Astrofisica Spaziale Fisica Cosmica, Palermo, Italy*
[3]*Istituto de Astrofisica de Andalucia (CSIC), Granada, Spain*
[4]*Center for Research and Exploration in Space Science And Technology (CRESST) and NASA Goddard Space Flight Center, Greenbelt MD 20771, USA*
[5]*Thüringer Landessternwarte Tautenburg, Sternwarte 5, 07778 Tautenburg, Germany*
[6]*Department of Physics and Astronomy, University of Nevada Las Vegas, Las Vegas, USA*
[7]*Space Research Institute (IKI), Moscow, Russia*
[8]*University of North Carolina at Chapel Hill, Chapel Hill, North Carolina, USA*
[9]*Pennsylvania State University, University Park, PA, USA*
[10]*Arizona State University, Tempe, Arizona, USA*
[11]*Instituto de Astrofísica, Facultad de Física, Pontificia Universidad Católica de Chile, 306, Santiago 22, Chile*
[12]*Millennium Institute of Astrophysics, Vicuña Mackenna 4860, 7820436 Macul, Santiago, Chile*
[13]*Centre for Astrophysics and Cosmology, University of Iceland, Reykjavik, Iceland*
[14]*Unidad Asociada Grupo Ciencia Planetarias UPV/EHU-IAA/CSIC, Departamento de Física Aplicada I, E.T.S. Ingeniería, Universidad del País Vasco UPV/EHU, Alameda de Urquijo s/n, E-48013 Bilbao, Spain.*
[15]*Ikerbasque, Basque Foundation for Science, Alameda de Urquijo 36-5, E-48008 Bilbao, Spain.*
[16]*Department of Physics, University of Maryland, Baltimore County, Baltimore, MD 21250, USA*
[17]*University of California Berkeley, USA*
[18]*University of California Santa Cruz, USA*
[19]*Universidad Nacional Autonoma de Mexico, Ciudad de Mexico, Mexico.*
[20]*The University of Chicago, IL, USA*
[21]*Crimean Astrophysical Observatory, 98409, pgt. Nauchny, Crimea*
[22]*Institute of Solar-Terrestrial Physics, Russian Academy of Sciences, 664033, p/o box 291; Lermontov st., 126a, Irkutsk, Russia*
[23]*Ulugh Beg Astronomical Institute, 100052, 33 Astronomicheskaya str., Tashkent, Uzbekistan*
E-mail: mdp@ifc.inaf.it

PoS(SWIFT 10)071

PROCEEDINGS OF SCIENCE

We present observations of GRB 130831A and its afterglow obtained with *Swift*, *Chandra*, and multiple ground-based observatories. This burst shows an uncommon drop in the X-ray light curve at about 10^5 s after the trigger, with a decay slope of $\alpha_X \simeq 7$. The standard Forward Shock (FS) model offers no explanation for such a behaviour. Instead, a model in which a newly born magnetar outflow powers the early X-ray emission is found to be more viable. After the drop, the X-ray afterglow resumes its decay with a slope characteristic of FS emission. The optical emission, on the other hand, displays no clear break across the X-ray drop and its decay is consistent with that of the late X-rays; we thus believe that the optical and late X-ray emission are both FS. We model our data to derive the kinetic energy of the ejecta and, in conjunction with the study of SN 2013fu associated with GRB 130831A, we work out for the first time the energy break-down of a supernova with a central engine into non-relativistic ejecta, relativistic ejecta that power the afterglow, and emission from the magnetar outflow.

Swift: 10 Years of Discovery,
2-5 December 2014
La Sapienza University, Rome, Italy

*Speaker.

1. Observations and results of data analysis.

The prompt emission of long GRB 130831A was detected by *Swift* BAT and *Konus − Wind*; its fluence (20-10000 keV) of 7.6×10^{-6} erg cm^{-2} at redshift z=0.48 [1] corresponds to an emitted energy of 1.1×10^{52} erg. *Swift* X-ray and UV/optical Telescopes (XRT, UVOT), SKYNET, RATIR, ISON, NOT, and GTC observed GRB 130831A up to $\simeq 10^7$ s after the trigger, covering the emission of SN 2013fu associated with this event [2]. These UVOIR observations span the range 160-1800 nm. In this work, we focus on the afterglow emission. At 10^5 s after the trigger, the X-ray light-curve begins a much faster decay. *Chandra* DDT observations (PI: De Pasquale) were carried out at +17 and +33 days, yielding 8 counts (5.4σ detection) and 1 count, respectively. Fig 1 shows the X-ray and UVOIR light-curves (LCs). We use the convention that flux density $F \propto t^{-\alpha}\nu^{-\beta}$; t is time from trigger and ν the frequency.

1.1 X-ray and UVOIR light-curves

We fit the X-ray LC with a power-law + broken power-law + power-law model, which yields an acceptable $\chi^2/dof = 51/48$. The steep break occurs at $98.3^{+3.0}_{-3.3}$ ks, and the slope of the preceding slow decay is $\alpha_2 = 0.80^{+0.01}_{-0.02}$. The 0.3–10 keV luminosity at 10 ks in the cosmological rest frame is $\simeq 10^{46}$ erg s^{-1}. The latest power-law slope is artificially shallow, to avoid an initial excessive flux. Thus, we fit the LC from 100 ks with a power-law + power-law model, obtaining a reasonable $\chi^2/dof = 2.4/3$. The slopes are $\alpha_3 = 6.8^{+2.0}_{-1.5}$ (3σ lower limit: 3.9), $\alpha_4 = 1.11^{+0.23}_{-0.29}$.
The early optical afterglow shows a flare followed by a plateau. At ~ 5 ks, a steeper decay begins. Optical data before 15 ks show deviations from a power-law decay and were not used for the fit. We fit the r', i' and R_C-band LCs, since we have measurements of the host galaxy flux in these filters, and we exclude the optical data between 230 ks and 6 Ms to avoid the contribution from SN 2013fu. The weighted average of the decay slopes in these three bands is $\alpha_{opt} = 1.58 \pm 0.03$. The LCs in the other filters are consistent with a simple power-law decay with this slope. No optical slope change is detected at the time of the X-ray flux drop.

1.2 Spectral energy distribution (SED)

The spectral energy distribution at 173 ks (Fig 2 bottom), after the end of the steep X-ray decay, was fitted by a simple power-law with spectral index $\beta_{OX} = 1.03 \pm 0.05$. We extrapolated the same fit model to 80 ks (Fig 2 top), i.e. before the steep X-ray break, by multiplying the normalization factor by $(173/80)^{1.58}$ and find that this extrapolation severely underestimates the X-ray flux. This result points to a different origin for the X-ray flux before the steep break.

2. Discussion

2.1 Origin of the emission: Forward Shock (FS) and internal dissipation components

In the FS model, the steepest decay is $\alpha \simeq p$, where p is the index of the power-law energy distribution of radiating electrons. However, $p \simeq 7$ is not predicted. Instead, after the 100 ks drop, the X-ray flux decay is consistent with the optical one, $\alpha_{opt} = 1.58$. The SED at 173 ks fits the two bands with a single power-law. All of this points to a common origin for the late emission in the

two bands. The FS model predicts that, in a constant density medium and below the synchrotron cooling frequency, the flux decay rate is $\alpha = 3/2\beta$; this is consistent with the observed values within 1σ. We find that other cases are excluded. We conclude that the early X-ray emission is produced by some dissipation mechanism(s) in the ejecta ("internal emission") which ceases at ~ 100 ks, causing a steep flux drop. The optical is basically always FS emission. Once the internal emission shuts off, the FS produces the X-ray late power-law decay, whose slope is consistent to that of the optical band. In the following, we briefly discuss a few models for the central engine of GRB 130831A in the light of the properties of the internal emission.

Newly born magnetar. The stellar progenitor of GRB 130831A may have collapsed into a magnetar, which powers jets via dipole spin-down. These jets may in turn produce the early X-ray emission of GRB 130831A [3]. In the basic scenario, the magnetar magnetic field and the X-ray luminosity are initially constant; but when the magnetar collapses into a black hole (BH) or uses up all its rotational energy, the flux drops. This model explains other bursts with an "internal plateau", such as GRB 070110 and GRB 060607A. However, it fails with GRB 130831A since the flux before the drop is not constant. In a more evolved version of this model, the magnetic field B decays with time as the angular speed. [4] found that, for an initial period P $\simeq 1$ ms and $B \simeq 10^{15}$ G, the jet luminosity, decay slope and duration are similar to those observed for GRB 130831A. The expected collapse of the magnetar into a BH, for the P and B parameters above, should take $\simeq 60$ ks (cosmological frame), again quite similar to the case of GRB 130831A.

Black hole with fall-back accretion disk. If the progenitor core collapses into a BH, stellar matter and ejecta failing to reach escape velocity may create an accretion disk. This system may power jets that produce the observed early X-ray emission. Once accretion is over, the emission drops. [5] envisaged two possibilities to explain the long X-ray plateau of GRBs like 130831A: *a)* The disk has low viscosity, and can last a few 10^4 s; however the predicted post-plateau decay is $\alpha \simeq 1.3$, much flatter than the $\alpha \simeq 7$ observed. *b)* The disk has high viscosity, and the jet luminosity follows the accretion rate. However, the stellar material needs to feed the disk for a few 10^4 s; the fall-back rate onto the disk is expected to evolve as $t^{-5/3}$, which is steeper than the observed $t^{-0.8}$ luminosity decay. Further, to explain the decay and the steep drop, angular momentum would need to be small in the outermost orbit, which is not predicted by stellar models.

Binary origin. A close binary formed by a compact object (e.g. a black hole) and a Wolf-Rayet star may have a common-envelope phase in which the compact object accretes from the companion, powering a jet that emits the observed X-rays [6]. For a compact object and a WR star mass of a few solar masses and standard viscosity, durations of a few 10^4 s are plausible. However, this scenario might suffer from the same problems as above, i.e. an inability to produce the steep decay and/or need of a peculiar structure of the WR star.

2.2 Energy partition of GRB 130831A and the associated SN2013fu.

The non-relativistic ejecta of SN 2013fu, the supernova associated with GRB 130831A, have kinetic energy of $E_{SN} = 1.9 \times 10^{52}$ erg [2]. Integrating the 0.3-10 keV luminosity of 130831A from the end of the prompt emission up to the steep drop, we find an X-ray energy release of $E_X = 2.9 \times 10^{50}$ erg. Knowing that the late flux is due to FS, we can infer the kinetic energy E_K of the relativistic ejecta [7]; we find $E_K = 11.8 \times 10^{52}$ erg. The energy emitted in prompt γ-rays is

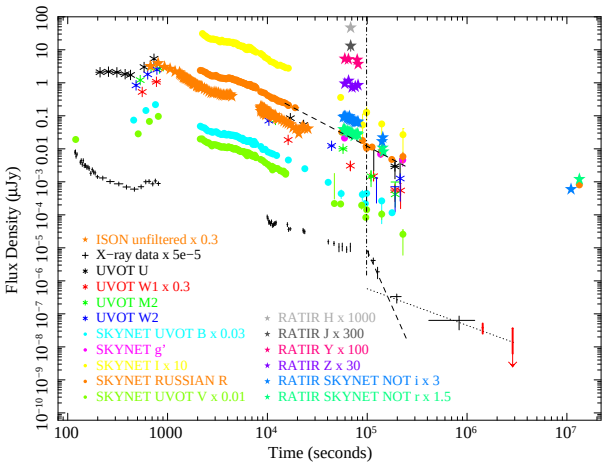

Figure 1: GRB 130831A UVOIR and X-ray light-curves. XRT and *Chandra* data points are black and red respectively. Data between 230 ks and 6000 ks are not shown because they are contaminated by SN 2013fu, associated with this GRB. The reader is referred to [2] for a complete study of the supernova. Data points at $\simeq 10^7$ s are due to the host galaxy. On to the *R* band and X-ray light-curves, we plot the best-fit power-law model (dotted and dashed lines). More specifically, the X-ray band model shows two power-laws that contribute to the flux. The vertical line indicates the fast decay of the X-ray light-curve, which has no counterpart in the optical.

$E_\gamma = 1.1 \times 10^{52}$ erg. The total energy budget of the GRB 130831A & SN 2013fu event sums up to $E_{tot} = 1.5 \times 10^{53}$ erg. However, E_γ, E_K and E_X estimated above are upper limits, valid only if the GRB emission is isotropic. If the outflow is collimated, they will decrease. The solid *Chandra* detection at 1.4×10^6 s enables us to set a minimum value on the opening angle of the outflow [8], $\theta \gtrsim 0.12$ rad, which in turn corresponds to a lower limit of the energy budget of $\simeq 2 \times 10^{52}$ erg. Moreover, if $\theta > 0.44$ rad then the budget is $> 3 \times 10^{52}$ erg, i.e. above the kinetic energy reservoir of a magnetar (magnetar limit). In Table 1, we show the breakdown of the energetics into the three different cases above.

3. Conclusions

The X-ray afterglow of the *Swift* GRB 130831A presents an initial shallow slope, which breaks to a steep decay with index $\alpha \simeq 7$ at 100 ks. The well-sampled optical afterglow shows no simultaneous break. The X-ray emission up to 100 ks cannot be produced by a typical FS and instead must be of "internal origin". A newly born magnetar with $P \simeq 1$ ms, $B = 10^{15}$ G may explain this X-ray emission, if its magnetic field decays with time.

The optical and the *late* X-ray emission (detected by *Chandra*) can be interpreted as FS emission, which enables us to derive the kinetic energy of the ejecta. We thus obtain the breakdown of the global energetics of GRB 130831A and its associated SN 2013fu and we show that, regardless of the unknown collimation of the explosion, at least 4.5% of the total energy is coupled with the relativistic ejecta, and less (probably much less) than 1% goes into X-ray emission of internal origin.

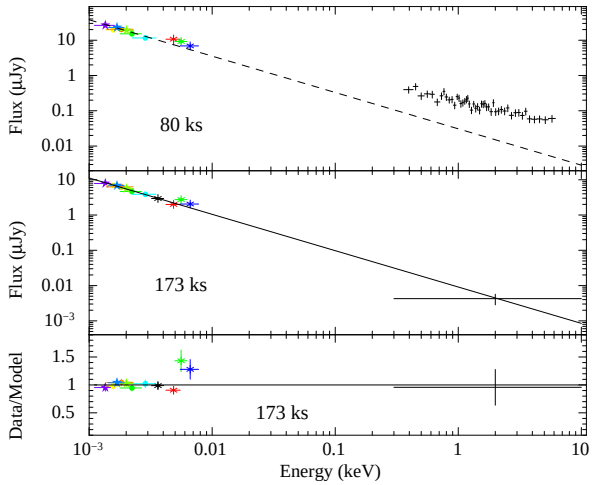

Figure 2: Spectral Energy Distributions (SEDs) of GRB 130831A at 80 ks (top) and 173 ks (2 days) after the trigger (bottom). We plot on the 173 ks SED the best-fit model, a power-law of index $\beta_{OX} = 1.03$. We rescale this model by $(173/80)^{1.58}$, where 1.58 is the temporal decay slope, and draw it on the 80 ks SED (dashed line). Such an extrapolation predicts the optical, but clearly underestimates the X-ray emission, which must be due to a component absent at 173 ks. Each filter has the same colour in both plots.

Correction Factor f_b^{-1}	$E_{\rm tot,52}$	$E_{\gamma,\rm corr}$	$E_{\rm X}$	$E_{\rm K}$
1 (isotropic)	14.8	7.1%	0.2%	80%
10 (magnetar limit)	3.2	3.3%	0.1%	37%
133 (upper limit)	2.0	0.4%	0.01%	4.5%

Table 1: Breakdown of the energetics of GRB 130831A and its associated SN 2013fu into energy emitted in γ-rays corrected for beaming ($E_{\gamma,\rm corr}$), energy produced in X-rays of internal origin $E_{\rm X}$, and kinetic energy associated with the relativistic GRB ejecta $E_{\rm K}$. The kinetic energy of the SN is $E_{\rm SN} = 1.9 \times 10^{52}$ (Cano et al. 2014), and the total energy is $E_{\rm tot} = E_{\rm SN} + E_{\gamma,\rm corr} + E_{\rm X} + E_{\rm K}$.

References

[1] A. Cucchiara et al., *GRB 130831A: Gemini North redshift.*, *GCN Circ.* (2013) 15144

[2] Z. Cano et al., *A trio of gamma-ray burst supernovae*, *A&A* **568** (2014) 19

[3] B. Zhang & P. Mészáros, *Gamma-Ray Burst Afterglow with Continuous Energy Injection: Signature of a Highly Magnetized Millisecond Pulsar*, *ApJL* **552** (2001) 35

[4] B. Metzger et al., *The protomagnetar model for gamma-ray bursts*, *MNRAS* **413** (2011) 2013

[5] P. Kumar, R. Narayan et al., *Mass fall-back and accretion in the central engine of gamma-ray bursts*, *MNRAS* **388** (2008) 1729

[6] M. Barkov & S. Komissarov, *Close binary progenitors of gamma-ray bursts*, *MNRAS* **401** (2010) 1644

[7] B. Zhang, et al., *GRB Radiative Efficiencies Derived from the Swift Data*, *ApJ* **655** (2007) 989

[8] W. Zhang & A. MacFadyen, *The dynamics of afterglow radiation of gamma-ray bursts. I. Constant Density Medium*, *ApJ* **698** (2009) 1261